ISSN 1674-1056
http://cpb.iphy.ac.cn
http://iopscience.iop.org/cpb
中国物理 B
Chinese Physics
中国物理 Chinese Physics B

Quantal studies of the sodium 3p←3s photoabsorption spectra perturbed by ground lithium atoms

N Lamoudi, F Talbi, M T Bouazza, M Bouledroua, K Alioua

Citation: Chin. Phys. B . 2019, 28(6): 063202. **doi:** 10.1088/1674-1056/28/6/063202
Journal homepage: http://cpb.iphy.ac.cn; http://iopscience.iop.org/cpb

What follows is a list of articles you may be interested in

Relativistic *R*-matrix calculations for *L*-shell photoionization cross sections of C Ⅱ

Lu-You Xie(颉录有), Qian-Qian Man(满倩倩), Jian-Guo Wang(王建国), Yi-Zhi Qu(屈一至), Chen-Zhong Dong(董晨钟)
Chin. Phys. B . 2018, 27(8): 083201. **doi:** 10.1088/1674-1056/27/8/083201

Pressure-broadened atomic Li(2s-2p) line perturbed by ground neon atoms in the spectral wings and core

Sabri Bouchoucha, Kamel Alioua, Moncef Bouledroua
Chin. Phys. B . 2017, 26(7): 073202. **doi:** 10.1088/1674-1056/26/7/073202

Low-lying electronic states of CuN calculated by MRCI method

Shu-Dong Zhang(张树东), Chao Liu(刘超)
Chin. Phys. B . 2016, 25(10): 103103. **doi:** 10.1088/1674-1056/25/10/103103

Influence of the interaction volume on the kinetic energy resolution of a velocity map imaging spectrometer

Peng Zhang(张鹏), Zheng-Peng Feng(冯正鹏), Si-Qiang Luo(罗四强), Zhe Wang(王哲)
Chin. Phys. B . 2016, 25(3): 033202. **doi:** 10.1088/1674-1056/25/3/033202

An *ab initio* investigation of the low-lying electronic states of BeH

Dong Yan-Ran, Zhang Shu-Dong, Hou Sheng-Wei, Cheng Qi-Yuan
Chin. Phys. B . 2012, 21(8): 083104. **doi:** 10.1088/1674-1056/21/8/083104

Quantal studies of sodium 3p ← 3s photoabsorption spectra perturbed by ground lithium atoms

N Lamoudi[1,2,†], F Talbi[1,3], M T Bouazza[1,4], M Bouledroua[1,3], and K Alioua[5,3]

[1] *Badji Mokhtar University, B. P.* 12 *Annaba, Algeria*
[2] *Laboratoire LESIMS*
[3] *Laboratoire de Physique des Rayonnements*
[4] *Laboratoire LAMA*
[5] *Souk-Ahras University, Souk-Ahras* 41000, *Algeria*

(Received 10 March 2019; revised manuscript received 18 April 2019; published online 29 May 2019)

The pressure broadening in the far wings, where the sodium Na (3p ← 3s) resonance line is perturbed by ground lithium Li (2s) atoms, has been theoretically analyzed. The NaLi potential–energy curves and the transition dipole moments are constructed by using a reliable *ab initio* data points to carry out the reduced-absorption coefficients $k_r(\nu, T)$. This quantum-mechanical investigation have demonstrated that the NaLi profile spectra show a satellite future in the red wing at wavelength $\lambda = 685$ nm in the temperature range 4000 K–1.8×10^4 K. The computation could also exhibit a second satellite, in the blue wing, near the wavelength $\lambda = 574$ nm beyond 6000 K and a third peak located at $\lambda = 490$ nm which begins to appear at 1.8×10^4 K.

Keywords: pressure broadening, absorption coefficient, satellite structure, radiative lifetime

PACS: 32.80.–t, 31.50.Bc, 31.50.Df, 32.70.Jz **DOI:** 10.1088/1674-1056/28/6/063202

1. Introduction

The study of the pressure broadening phenomena in the far wings of the emission and absorption spectra of the gaseous mixture has in recent years gained a lot of attention from theoretical physicist, spectroscopisist and astrophysicist. In fact, such broadening is arrise from the interactions of radiator atom, molecule or ion with the neighboring particles of the gas or plasma. Accurate simulations or measurements of the collisionally broadened spectra lines and the knowledge of the possible satellite peak positions can provide informations on the atom-atom interaction, temperature, density and composition of the gas studied.[1,2] Furthermore after the discovery of brown dwarfs and extrasolar giant planets which their atmosphere are dominated by alkli-metal,[3–6] the pressure broadened line profile of alkli-metal atoms perturbed by parent or foreign atoms, have been of particular in the last two decades extensively studied by theoretical[5–10] and experimental[11–14] groups.

The aim of this investigation is to determine quantum mechanically the sodium–lithium (NaLi) photoabsorbtion spectra, while the radiating Na (3p ← 3s) atoms are perturbed by the ground lithium Li (2s) atoms. For this purpose we will first construct carefully the Na (3s) + (2s) and Na (3p) + Li (2s) potential–energy curves (PECs) and the required transition dipole moments (TDMs). We will thereafter attempt to evaluate the quality of the constructed (PECs) and (TDMs) through the computation of the NaLi ro-vibrational levels of each electronic molecular states and the radiative lifetimes of the excited states. The constructed NaLi (PECs) and (TDMs) will be then used to carry out the reduced-photoabsorption coefficients $k_r(\nu, T)$ to analyze the satellite futures (intensity and position) in the far wings, and to look at the effect of temperature on the shape of the spectra.

2. Theory

The pressure broadening of the sodium (3p ← 3s) resonance absorption line, when the radiating Na (3s/3p) interacting with ground lithium Li (2s) atoms, is attribute to the singlet transitions from the NaLi ground state $X\ ^1\Sigma^+$ to the first $A\ ^1\Sigma^+$ and $B\ ^1\Pi$ excited molecular symmetries, and to the triplet transitions from the ground $a\ ^3\Sigma^+$ state to the excited $b\ ^3\Pi$ and $c\ ^3\Sigma^+$ states. From molecular spectroscopy[1,2] it is well known that during any photoabsorption process, the transitions from one ground molecular symmetry to the corresponding excited state are governed, in general by four types of transitions namely, bound–bound (bb), bound–free (bf), free–bound (fb), and free–free (ff). For the case of the NaLi quasimolecule, as it will be seen in the next section, the singlet $X\ ^1\Sigma^+$, $A\ ^1\Sigma^+$, and $B\ ^1\Pi$ states are quite bound, both transitions $A \leftarrow X$ and $B \leftarrow X$ are then expected to contribute with the all possible transitions. Concerning the triplet transitions, the ground $a\ ^3\Sigma^+$ potential curve has a deeper well, whereas the excited $b\ ^3\Pi$ and $c\ ^3\Sigma^+$ curves are purely repulsive we then consider solely the bound–free and free–free transitions of the $c \leftarrow a$ and $b \leftarrow a$

†Corresponding author. E-mail: noralamoudi@yahoo.fr

contributions. The pressure broadening phenomena in the far wing photoabsorption spectra of sodium Na (3p←3s) caused by lithium perturber, is described for an absorbed frequency ν and at a given temperature T, by the reduced-photoabsorption coefficient $k_r(\nu,T)$ which should be the sum of the four absorption coefficients corresponding to different types of transitions. In this study, we adopt the reduced-photoabsorption coefficients formula of Chung *et al.*[15,16] which have been given in detail in our previous works.[17,18] If we denote by double and single prime the initial and final states, and assuming that $J' \simeq J'' = J$ where J is the total angular momentum, the free–bound reduced-absorption coefficient for transitions from the all lower continuum $(\varepsilon'' J\Lambda'')$ to a set of ro-vibrational levels of the upper states $(v'J\Lambda')$ is[16]

$$k_r^{\rm fb}(\nu,T) = \frac{8\pi^3\nu}{3c}\varpi\left[\frac{2\pi\hbar^2}{\mu k_{\rm B}T}\right]^{3/2}\sum_{v'J}(2J+1)\left\langle\Phi_{\varepsilon''J\Lambda''}(R)\left|D(R)\right|\Phi_{v'J\Lambda'}(R)\right\rangle^2\exp\left(-\frac{\varepsilon''}{k_{\rm B}T}\right), \tag{1}$$

where v is the vibrational quantum numbers, Λ is the axial component of the total electronic orbital angular momentum, ε is the energy of the free states, and ϖ represents the probability that the sodium and lithium atoms form a molecule in the lower electronic state.

Likewise, the reduced absorption coefficients corresponding to the remaining type of transitions are given by the following set of expressions

$$k_r^{\rm bf}(\nu,T) = \frac{8\pi^3\nu}{3c}\varpi\left[\frac{2\pi\hbar^2}{\mu k_{\rm B}T}\right]^{3/2}\sum_{v''J}(2J+1)\left\langle\Phi_{v''J\Lambda''}(R)\left|D(R)\right|\Phi_{\varepsilon'J\Lambda'}(R)\right\rangle^2\exp\left(-\frac{E_{v''J\Lambda''}}{k_{\rm B}T}\right), \tag{2}$$

$$k_r^{\rm ff}(\nu,T) = \frac{8\pi^3\nu}{3c}\varpi\left[\frac{2\pi\hbar^2}{\mu k_{\rm B}T}\right]^{3/2}\sum_{J}\int{\rm d}\varepsilon'(2J+1)\left\langle\Phi_{\varepsilon''J\Lambda''}(R)\left|D(R)\right|\Phi_{\varepsilon'J\Lambda'}(R)\right\rangle^2\exp\left(-\frac{\varepsilon''}{k_{\rm B}T}\right), \tag{3}$$

$$k_r^{\rm bb}(\nu,T) = \frac{1}{h}\frac{8\pi^3\nu}{3c}\varpi\left[\frac{2\pi\hbar^2}{\mu k_{\rm B}T}\right]^{3/2}\sum_{v''J}\sum_{v'}g(\nu-\nu_{\rm tr})(2J+1)\left\langle\Phi_{v''J\Lambda''}(R)\left|D(R)\right|\Phi_{v'J\Lambda}(R)\right\rangle^2\exp\left(-\frac{E_{v''J\Lambda''}}{k_{\rm B}T}\right). \tag{4}$$

The function of the form $g(\nu-\nu_{\rm tr})$ appearing in Eq. (4) is approximated in this computation by the inverse of the frequency bin size $\Delta\nu$ and $\nu_{\rm tr}$ is the transition frequency defined by

$$h\nu_{\rm tr} = E_{v'J\Lambda'} - E_{v''J\Lambda''} + h\nu_0, \tag{5}$$

here $E_{vJ\Lambda}$ is the ro-vibrational energie levels and ν_0 is the Na (3s–3p) atomic transition frequency.

In the matrix elements $\left\langle\Phi_{\varepsilon J\Lambda}\left|D(R)\right|\Phi_{vJ\Lambda}\right\rangle$ the symbols $D(R)$, defined each internuclear separation R, means the electronic transition dipole moment that connect the lower and upper states involved in the allowed transitions, $\Phi_{\varepsilon J\Lambda}$ and $\Phi_{vJ\Lambda}$ are respectively the energy- and space-normalized radial wave functions, determined by solving numerically the radial wave equation

$$\frac{{\rm d}^2\Phi(R)}{{\rm d}R^2} + \frac{2\mu}{\hbar^2}\left[\mathscr{E} - V(R) - \frac{\hbar^2}{2\mu}\frac{J(J+1)-\Lambda^2}{R^2}\right]\Phi(R) = 0, \tag{6}$$

the interatomic potential energy $V(R)$ is measured with respect to the dissociation limit, and the energy $\mathscr{E} = \varepsilon$ is positive for continuous free states and $\mathscr{E} = E_{vJ\Lambda}$ is negative for discrete bound states.

3. Molecular data

To be able to carry out the reduced-absorption coefficients for the NaLi system we must construct carefully the potential-energy curves for the considered molecular states and the transition dipole moments for allowed transitions.

3.1. Potential energy curves (PECs)

The molecular symmetries through which a ground sodium atom Na (3s) interacts with a ground Li (2s) are the singlet $X\ ^1\Sigma^+$ or the triplet $a\ ^3\Sigma^+$ states. When the sodium atom is in the first excited state Na (3p) and interact with the ground Li (2s), the two atoms form a quasimolecule in one of the four $A\ ^1\Sigma^+$, $B\ ^1\Pi$, $b\ ^3\Pi$, and $c\ ^3\Sigma^+$ excited molecular states. To build the above six states in the entire range of interatomic distance R we used, in the intermediate region going from $3.2a_0$ to $19a_0$ the accurate *ab-initio* data points provided to us by Aubert–Frécon M.[19] We completed the potential energy curves analytically at the short-range $(R \leq 3.2a_0)$ and the long-range $(R \geq 19a_0)$ by using the Born Mayer Potential $V_{\rm SR}(R) = \alpha\exp(-\beta R)$[20] and the dispersion potential $V_{\rm LR}(R) = -\sum_n C_n/R^n$, respectively. Where α and β are two constant parameters that have been computed by fitting and listed in Table 1, and the C_n $(n = 6, 8, 10)$ are the dispersion coefficients given by Marinescu and Sadeghpour.[21] These coef-

ficients are for the $^{1,3}\Sigma^+$ ground states, $C_6 = 1.459 \times 10^3$, $C_8 = 9806 \times 10^4$ and $C_{10} = 91276 \times 10^6$, while for the excited $^{1,3}\Sigma^+$ molecular states $C_6 = 10648 \times 10^3$ and $C_8 = 13333 \times 10^4$ and for the $^{1,3}\Pi$ ones $C_6 = 10849 \times 10^3$ and $C_8 = 1199 \times 10^4$. The constructed Na (3s/3p) + Li (2s) (PECs) are plotted and compared with computed data of Schmidt *et al.*[22] in Fig. 1.

Table 1. Potentials short-range constant parameters (in unit a.u. The unit a.u. is short for atomic unit).

Constant parameters	NaLi molecular states					
	X $^1\Sigma^+$	$a\,^3\Sigma^+$	A$^1\Sigma$	B$^1\Pi$	$b\,^3\Pi$	$c\,^3\Sigma^+$
α	47.879	1.6245	2.4471	1.86563	1.7312	1.86569
β	2.22765	0.87182	1.0411	0.93505	0.863743	0.878159

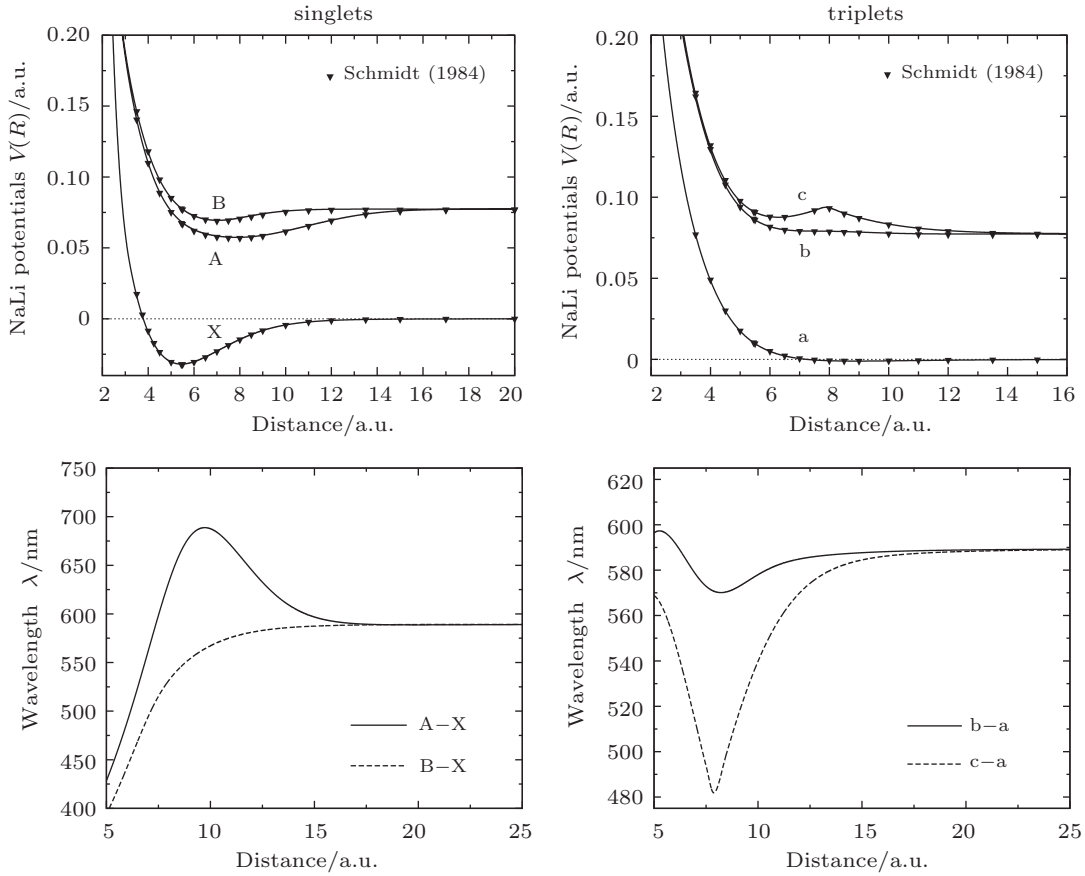

Fig. 1. Na (3s) + Li (2s) and Na (3p) + Li (2s) potential–energy curves $V(R)$ (upper graphes) and potential-differences (lower graphes) *versus* internuclear separation (R). All singlet and triplet curves are compared with *ab-initio* data from Schmidt-Mink I *et al.*[22] The potential differences are converted into wavelengths.

The overall agreement is seen to be good. The spectroscopic constants such as dissociation energy D_e, the equilibrium position R_e, and the minimum-to-minimum electronic excitation energy T_e, derived from our constructions are assembled in Table 2 and compared with theoretical data of Schmidt–Mink I *et al.*,[22] Mabrouk N and Berriche H,[23] and Petsalakis I D *et al.*,[24] and measured values of Kappes M M *et al.*[25] In the present constructions the triplet excited states $b^3\Pi$ and $c^3\Sigma^+$ are both found to be predominantly repulsive. Two another theoretical investigations[23,24] revealed that these two states are mainly repulsive. Furthermore, we have in particular plotted in panel (b) of Fig. 1 the potential differences $V_{A-X}(R)$, $V_{B-X}(R)$, $V_{b-a}(R)$, and $V_{c-a}(R)$. According to the semiclassical theory,[2] a satellite structure is expected to be observed in the absorption spectra when the potential-difference curves presents an extremum. The position of such extremum, converted in terms of the wavelengths, predicted the position of the possible satellites. Therefore, the curve in Fig. 1(b), predicts that one satellite future should appear in the red wing from the $A \leftarrow X$ transitions close to the wavelength $\lambda \sim 686$ nm. Two others satellites are expected to be occurred in the blue wing, one from the $b \leftarrow a$ transitions near the wavelength $\lambda \sim 569$ nm and the second from the $c \leftarrow a$ transitions at approximately $\lambda \sim 482$ nm.

Table 2. Comparison of the spectroscopic constants of the ground and excited NaLi potentials with experimental and theoretical values.

Molecular states	D_e/cm^{-1}	R_e/a_0	T_e/cm^{-1}	References
$X\ ^1\Sigma^+$	7005.83	2.883	–	this work
	7057	2.89	–	Ref. [22]theor.
	7054	2.873	–	Ref. [23]theor.
$a\ ^3\Sigma^+$	237.761	4.720	6768	this work
	220	4.720	6834	Ref. [22]theor.
	216	4.754	6841	Ref. [23]theor.
$A\ ^1\Sigma^+$	4361.32	4.166	19613.825	this work
	4377	4.133	19601(±20)	Ref. [22]theor.
	3867	–	–	Ref. [24]theor.
	4341	4.164	–	Ref. [23]theor.
	5424	3.59	18600(±10)	Ref. [25]exp.
$B\ ^1\Pi$	1726.94	3.729	22248.205	this work
	1724	3.758	22295(±3)	Ref. [22]theor.
	1450	–	–	Ref. [24]theor.
	1722	3.725	22300	Ref. [23]theor.
	1762(±2)	2.78	22262(±2)	Ref. [25]exp.

3.2. Transition dipole moments (TDMs)

Following the same way that used early for constructing the potential–energy curves, we constructed the singlets and triplets transition dipole moments $D(R)$ related to the transition from the ground states to the excited ones. In fact we used in the intermediate range of interatomic distances the *ab-initio* data points provided for us by Aubert-Frecon M.[19] The foregoing data are smoothly connected in the long range to the formula proposed by Chu and Dalgarno[27] $D(R) \sim D_\infty + AR^{-3}$. Here, the constant A and the asymptotic value D_∞ are determined by fitting the long range (TDMs) data points to a form analogous to the last equation. Our fitting give $D_\infty = 2.533$, $A = -2790.76$ for the Σ–Σ transitions and $A = -2790.76$ for the Σ–Π transitions. In the short range region the transition dipole moments $D(R)$ follow the linear form $D(R) \sim a + bR$. Both parameter a and b are given by the continuity conditions of the $D(R)$ function. The found values are compiled in Table 3.

Table 3. Constant parameters adopted for the constructed singlets and triplets transition dipole moments $D(R)$.

	Transitions			
	ΣΣ		ΣΠ	
	Singlets	Triplets	Singlets	Triplets
a	2.192	0.964	1.781	0.831
b	−0.210	−6.494	−0.262	0.266

Transition dipole moments $D(R)$ against internuclear separation (R) are shown in Fig. 2.

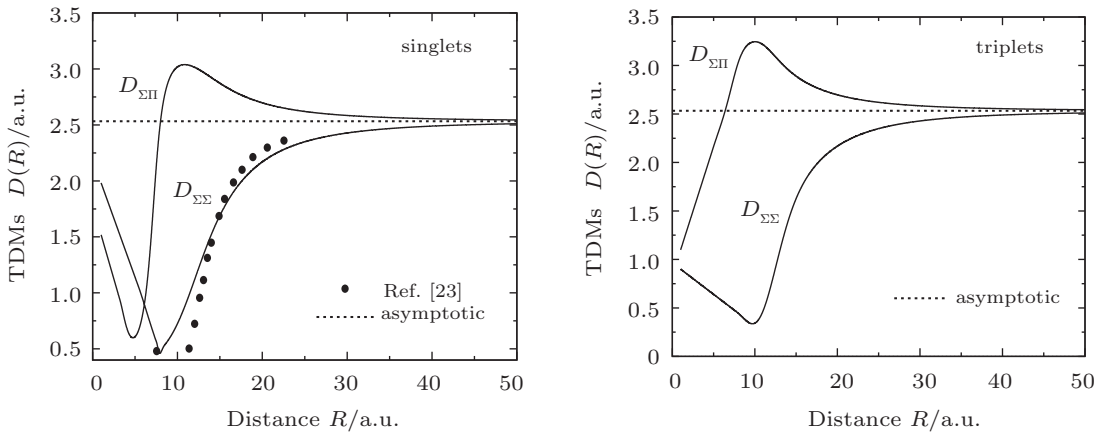

Fig. 2. Transition dipole moments $D(R)$ against internuclear separation (R). The singlet $D_{\Sigma\Sigma}$ (TDMs) are compared with *ab-initio* data from Mabrouk N and Berriche H.[23]

4. PECs and TDMs assessments

We assess the quality and accuracy of the constructed potential–energy curves and transition dipole moments by calculating the ro-vibrational energy levels and their radiative lifetimes.

4.1. Vibrational levels

The ro-vibrational energy levels of the singlet and triplet Na (3s/3p) + Li (2s) states, are determined by solving numerically the the radial wave equation (Eq. (6)). To achieve the goal, we adapted, with some important modifications, the subcode ALF (Automatic Levels Funder) of LeRoy's package Level version 7.4.[28] Our calculation yields to the 48 levels for both of the $X^1\Sigma^+$ and $A^1\Sigma^+$ states, 16 for the $B\ ^1\Pi$ state and 13 for the triplet ground state $a\ ^3\Sigma^+$. The corresponding values of the binding energies $E(v,J)$ with $J = 0$ for all the Σ^+ states and $J = 1$ for the Π ones are compared with theoretical data of Schmidt-Mink I *et al.*[22] as listed in Table 4. We should note here that the present computation discloses 1 quasibound level for the $b\ ^3\Pi$ state and 7 for the $c\ ^3\Sigma^+$ molecular state.

Table 4. Rotationl-vibrational energy levels $E(v,J)$, in unit cm^{-1}, for the NaLi molecular states calculated with respect to their minimum. $J = 0$ and $J = 1$ for Σ and Π states respectively.

	$X\ ^1\Sigma^+$			$A\ ^1\Sigma^+$		$B\ ^1\Pi$		$a\ ^3\Sigma^+$	
v	This work	Ref. [22]	Ref. [26]	This work	Ref. [22]	This work	Ref. [22]	This work	Ref. [22]
0	126.30	128	128.1	53.68	53	77.10	75	20.43	20
1	376.76	381	381.7	161.20	159	228.41	224	58.50	56
2	624.07	632	632.0	269.10	266	376.40	370	92.84	89
3	868.12	879	878.9	377.32	373	520.10	511	123.41	119
4	1108.89	1122	1122.4	485.83	481	659.24	648	150.15	144
5	1346.38	1362	1362	594.55	590	792.70	781	172.93	166
6	1580.53	1599	1598.9	703.40	698	922.20	908	191.76	184
7	1811.30	1832	1831.9	812.32	807	1044.75	1029	206.60	198
8	2038.64	2062	2061.3	921.23	916	1160.80	1145	217.63	207
9	2262.50	2288	2287.2	1030.04	1025	1269.10	1253	225.63	
10	2483.0	2511	2509.4	1138.70	1134	1371.10	1354	231.58	
11	2670.0	2730	2728.0	1247.10	1243	1463.80	1447	231.60	
12	2913.0	2945	2942.9	1355.20	1351	1546.95	1531	235.83	
13	3122.04	3156	3154.0	1462.88	1459	1618.61	1604	237.63	
14	3327.61	3363	3361.3	1570.13	1567	1678.70	1666		
15	3529.29	3567	3564.2	1676.90	1674	1673.90	1714		
16	3727.01	3766	3764.2	1783.10	1781	–	1737		
17	3920.66	3961	3959.7	1888.56	1888				
18	4110.15	4152	4151.1	19993.40	1993				
19	4295.36	4338	4338.2	2097.50	2098				
20	4476.20	4520	4521.1	2200.70	2202				
21	4652.50	4698	4699.5	2303.10	3206				
22	4824.16	4870	4873.3	2404.50	2408				
23	4991.01	5038	5042.4	2504.96	2510				
24	5153.00	5201	5206.6	2604.40	2610				
25	5309.65		5365.7	2702.60					

4.2. Radiative lifetimes

The purpose here is to calculate the radiative lifetimes of the both exited states $A\ ^1\Sigma^+$ and $B\ ^1\Pi$ of the NaLi dimer. In the framework of the quantum theory, the radiative lifetime τ of the transition from the upper bound level $(v'J\Lambda')$ of the exited state to all the lower continuum $(\varepsilon''J\Lambda'')$ and bound $(v''J\Lambda'')$ levels of the corresponding ground states, is defined as being the inverse of the sum of the spontaneous bound–free and bound–bound emission rates $A(v'J\Lambda)$,[29,30] then

$$\tau = \frac{1}{\mathscr{A}(v'J\Lambda)}, \tag{7}$$

with

$$\mathscr{A}(v'J\Lambda) = \frac{64\pi^4}{3hc^3}\frac{2-\delta_{0,\Lambda'+\Lambda''}}{2-\delta_{0,\Lambda'}}\left[\int_0^\infty \nu^3_{v'J\Lambda',\varepsilon''J\Lambda''}\left\langle \Phi_{v'J\Lambda'}(R)\left|D(R)\right|\Phi_{\varepsilon''J\Lambda''}(R)\right\rangle^2 \mathrm{d}\varepsilon'' + \sum_{v''}\nu^3_{v'J\Lambda',v''J\Lambda''}\left\langle \Phi_{v'J\Lambda'}(R)\left|D(R)\right|\Phi_{v''J\Lambda''}(R)\right\rangle^2\right]. \tag{8}$$

Table 5 gives some of $A\ ^1\Sigma^+$ and $B\ ^1\Pi$ radiative lifetime values obtained by computations. To our knowledge, no measured or computed lifetime values are available in literature for comparison. Normally the lifetime of the highest rotationless vibrational states near to the dissociation limit should be close to the atomic lifetime of isolated Na atom. Therefore, we have evaluated the sodium atomic 3s–3p lifetime τ_a by using the following weighted sum

$$\frac{1}{\tau_a} = \frac{1}{3}\mathscr{A}(v'_{\max}00) + \frac{2}{3}\mathscr{A}(v'_{\max}01).$$

Our value 16.80 ns does not exceed a difference of 0.5 ns from the experimental values 16.3 ± 0.1 ns found by Reho *et al.*,[31] 16.35 ns of Carlsson and Sturesson,[32] 16.3 ns given by Volz and Schmoranze,[33] and 13.31 ns of Tiemann, *et*

al.[34]

Table 5. Radiative lifetimes (in unit ns) of some ro-vibratoinal levels of the NaLi $A^1\Sigma^+$ and $B^1\Pi$ states.

v'	J'						
	0	10	20	30	40	50	60
				$A\,^1\Sigma^+(\Lambda'=0)$			
0	445.06	458.20	446.60	478.84	492.52	504.47	511.64
10	916.86	258.19	258.469	301.69	267.50	273.24	281.13
20	578.95	184.67	183.56	206.02	148.16	183.88	183.52
30	337.04	126.19	124.44	133.40	120.42	116.98	112.35
40	176.76	73.06	71.01	73.14	64.17	58.69	51.11
42	150.027	62.59	60.48	56.93	46.86	46.29	36.23
44	119.38	51.98	49.75	40.24	40.51	30.87	
46	92.23	4640.97	38.40	23.96	33.01		
47	69.88	34.84	31.86				
				$B\,^1\Pi(\Lambda'=1)$			
0	21.19	21.06	20.701	20.13	19.381	18.49	17.50
5	64.60	16.26	16.06	15.75	15.34	14.83	14.24
10	53.58	13.56	13.41	13.17	12.84	12.40	11.77
11	51.74	13.12	12.98	12.74	12.41	11.94	
12	49.92	12.72	12.57	12.33	11.98		
13	48.12	12.34	12.19	11.95	11.56		
14	45.66	11.99	11.85	11.60			
15	12.31	11.76					

5. Reduced-absorption coefficients

To determinate the NaLi photoabsoption spectra and the effect of temperature, we have carried out the fb, bf, ff, and bb reduced-absorption coefficients by using the above equations (1)–(4). By adopting the Numerov algorithm,[35] we solved numerically the radial wave equation Eq. (6), which allowed us to determine the normalized wave functions and the corresponding energies required in the calculation of the matrix elements $\langle \Phi_{\varepsilon J\Lambda} | D(R) | \Phi_{vJ\Lambda} \rangle$.

For the computation of the free–free integral appearing in Eq. (3) we used the Gauss–Laguerre quadratureu[36] with 100 weighted points. In the aim to simulate accurately the NaLi photoabsorption profile we have performed the calculations for wavelengths interval going from 350 nm to 750 nm with a frequency step $\Delta\nu = 10$ cm^{-1} and by taking the maximum values of the rotational quantum number $J_{\max} = 500$ for the free–free transitions and $129 \leq J_{\max} \leq 239$ for the remaining transitions. Moreover all the bound and quasibound levels are including in the calculations.

The profile spectra, around the Na (3s⟵ 3p) resonance line $\lambda_0 = 589$ nm, in the presence of Lithium atoms, obtained by our full quantum mechanical computation for four temperatures, namely $T = 2.0\times10^3$, 6.0×10^3, 1.0×10^4, and 1.4×10^4 K are plotted in Fig. 3.

The column (a) in Fig. 3 shows the $A \leftarrow X$, $B \leftarrow X$, $b \leftarrow a$, and $c \leftarrow a$ reduced-absorption coefficients. Column(b) presents the sum of all the contributions. From these curves, one may observed, in particular, that the both singlet transitions $A \leftarrow X$ and $B \leftarrow X$ dominate the general shape of the total spectra. In fact the $A \leftarrow X$ bands are the principal component in the red wing and contribute also to the blue branches, whereas the $B \leftarrow X$ transitions contribute solely and strongly to the blue wing.

One may notice that both $A \leftarrow X$ and $B \leftarrow X$ reduced-absorption coefficients decrease considerably in magnitude with increasing temperatures. The intensity decrease of the blue wing of the $A \leftarrow X$ transitions is more severe. The $A \leftarrow X$ transitions generate one satellite structure in far-red wing around the wavelengths $\lambda = 685$ nm, this red satellite result from the bound–bound and free–free transitions, as it can be seen in the insert of Fig. 3, and it is present in the total spectra for all studied temperatures.

The column (a) in Fig. 3 revealed that the triplet $c \leftarrow a$ and $b \leftarrow a$ transitions constitute a minor contributions compared with the singlet spectra. In other words their contribution is restricted to the creation of the satellites in the blue wing. Indeed the $b \leftarrow a$ transitions participate with one satellite close to the $\lambda = 574$ nm which become visible in the total spectra beyond $T \geq 6000$ K. Likewise the $c \leftarrow a$ transitions generate one satellite in the vicinity of the wavelength $\lambda = 490$ nm. The latter satellite do not appears on the total spectra for all temperature previously cited. According to the Fig. 3 column (a) the intensity of the satellite under consideration at $T = 2000$ K is about a factor of 10^4 less than of the $A \leftarrow X$ and $B \leftarrow X$ transitions intensities. As stated above, the intensity spectrum of the $A \leftarrow X$ transitions diminishes when the temperature increases and becomes, at $T = 1.4\times10^4$ K, of the same order of magnitude than the intensity corresponding to the $c \leftarrow a$ transitions, whereas the $B \leftarrow X$ transitions intensity remains high compared with the $c \leftarrow a$ transitions ones.

We have also carried out the NaLi reduced-absorption coefficients for more high temperatures. We represent in Fig. 4 the total spectra and those corresponding to the four partial transitions at $T = 1.6\times10^4$ K and 1.8×10^4 K. At such temperatures the $B \leftarrow X$ spectrum intensity decreases again and becomes comparable with the $c \leftarrow a$ transitions intensity the satellite at 490 nm begins then to emerge. From the above discussion, We recap that the NaLi photoabsorption spectra exhibit in the red wing an apparent satellite, at all temperatures, in the vicinity of the wavelength $\lambda \sim 685$ nm, while the blue wing shows beyond $T \geq 6000$ K a second satellite located at $\lambda = 574$ nm and a third one at approximately $\lambda = 490$ nm which starts to appear in the global spectra at $T = 1.8\times10^4$ K. All the positions of the above sattelites agree quite well with the wavelength values found earlier from the classical method.

In order to examine the behavior of the satellite intensity and positions with temperature, we present in Fig. 5 the satellite peaks appearing at the wavelengths 685, 574, and 490 nm for temperature range 2000 K–1.4×10^4 K. Figure 5(a) reveals that the amplitude of satellite peak that appear at 685 nm diminishes, almost, with a factor of 10^2 when the temperature goes from 2000 K to 6000 K. Beyond this temperature the peak intensity change without reacheing 10%. We think that the reason for this strong lowering is due to the fact that this satellite arises bassically from bound–bound transitions, at higher temperature the lower ro-vibrational levels are less populated. In the range of 6000 K to 1.4×10^4 K, the temperature has no influence on the intensity satellite peaks occurring in the positions 574 nm and 490 nm resulting from the triplet $c \leftarrow a$ and $b \leftarrow a$ transitions respectively, as we can easily seen in Fig. 5(b) and Fig. 5(c). As well, from Fig. 5 one may notice that is no influence of temperature on the position of the satellites.

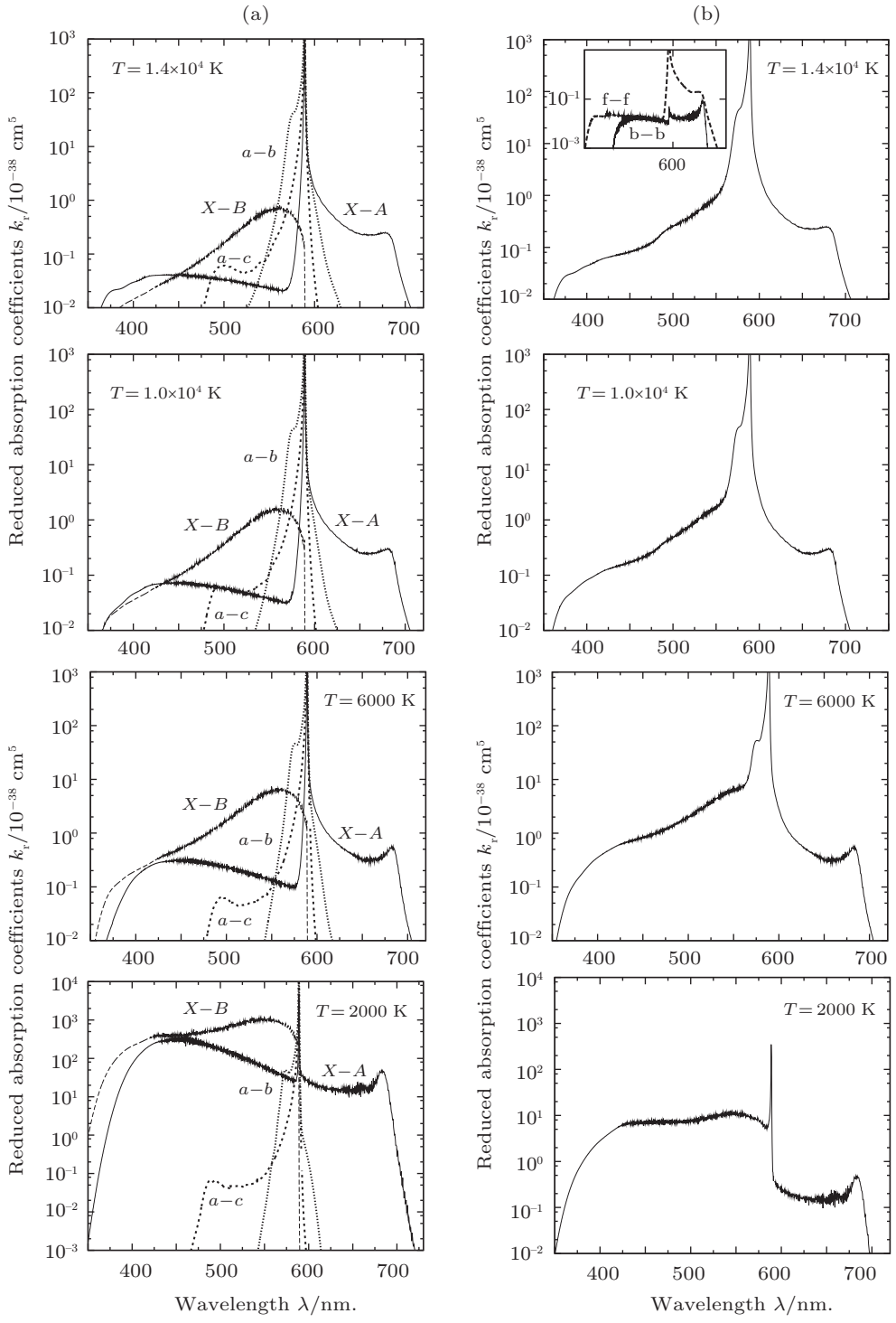

Fig. 3. NaLi full quantum-mechanical reduced-photoabsoption coefficients for temperature range 2000 K–1.4×10^4 K. Part (a) shows the details of the $A \leftarrow X$, $B \leftarrow X$, $b \leftarrow a$, and $c \leftarrow a$ transitions. Part (b) represents the sum of all the previous contributions. The insert displays the bound–bound and free–free $A \leftarrow X$ transitions around the red wing satellite positions.

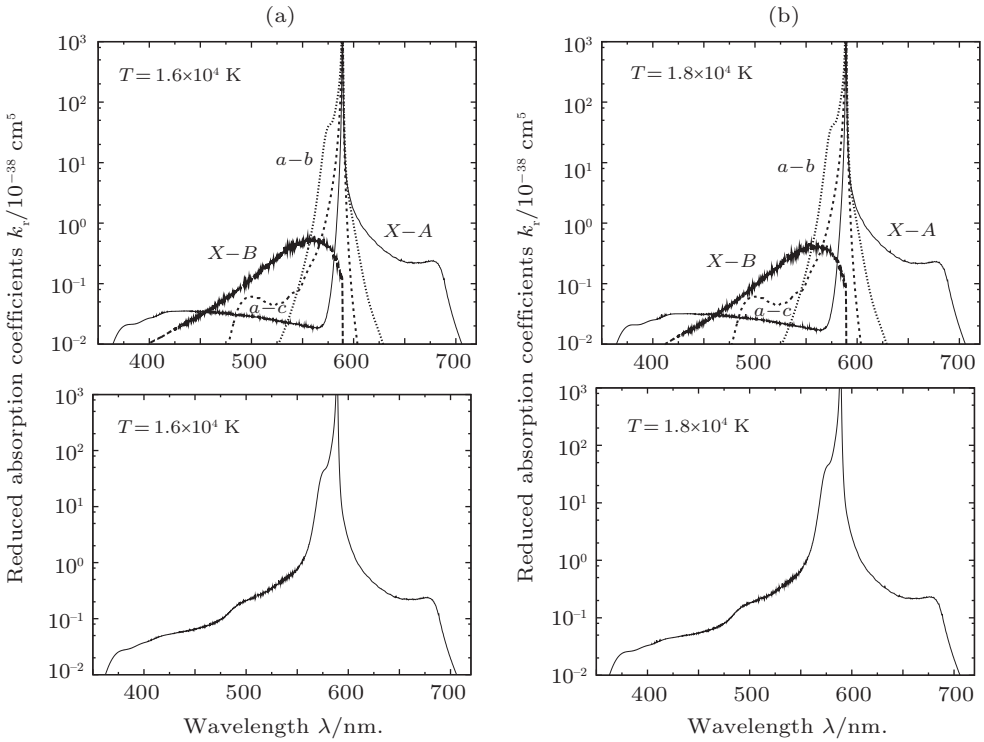

Fig. 4. NaLi full quantum-mechanical reduced-photoabsoption coefficients for temperatures 1.6×10^4 K and 1.8×10^4 K. The upper row shows the details of the different transitions and the lower row represents the sum of the all contributions.

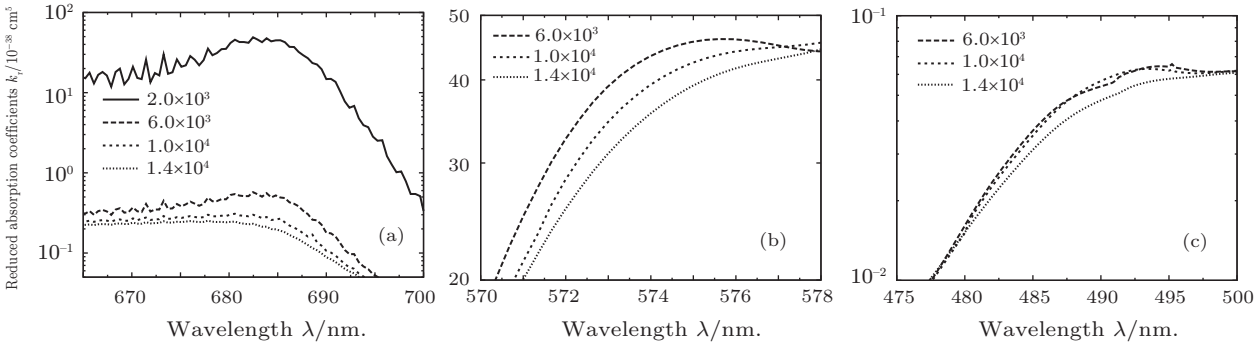

Fig. 5. Temperature effect on the position and intensity of the satellite peaks. Panel (a) shows the red wing satellite near 685 nm. Panels (b) and (c) represent the blue wing peaks located around 574 nm and 490 nm respectively.

6. Conclusion

We have determined theoretically the pressure-broadening spectrum of radiator sodium atom interacting with perturbed lithium. The needed potential–energy curves and transition dipole moments are constructed upon purely *ab-initio* data points. Their reliability is assessed by determining the ro-vibrational levels and the radiative lifetimes of the NaLi excited states. The results showed an important effect of temperature on the far wings and the profile is found dominate by the singlet transitions. Our calculations revealed that the photoabsorbtion spectra display, three satellite structures close to 685 nm in the red wing and 574 nm and 490 nm in the blue wing. The first satellite generated by the $A \leftarrow X$ transitions occurred at all interested temperatures. Whereas the second one given by the $c \leftarrow a$ bands appears at beyond $T \gtrsim 6000$ K and the third peak due to the $b \leftarrow a$ transitions emerges at approximately $T = 1.8\times10^4$ K.

Acknowledgments

The authors are very grateful to Aubert-Frécon Monic for all the data points she provided us.

References

[1] Allard N F and Kielkopf J F 1982 *Rev. Mod.* **54** 1103
[2] Szudy J and Baylis W E 1996 *Phys. Rep.* **266** 127
[3] Burrows A, Hubbard W, Lunine J I and Liebert J 2001 *Rev. Mod. Phys.* **73** 719
[4] Hawley S L 2001 *Proceedings of the* 12*th Cambridge Workshop on cool Stars. Stellar Systems, and the Sun*, 30 July–3 August 2001 (University of Colorado USA) p. 97
[5] Allard N F, Allard F, Hauschildt P H, Kielkopf J F and Machin L 2003 *Astrom. Astrophys.* **411** L473
[6] Allard N F, Allard F and kielkopf J F 2005 *Astrom. Astrophys.* **440** 1195
[7] Allard N F and Spiegelman F 2006 *Astrom. Astrophys.* **452** 351

[8] Mullamphy D F T, Peach G, Venturi V, Whittingham B and Gibson S J 2007 *J. Phys. B* **40** 1141
[9] Zhu C, Babb J F and Dalgarno A 2005 *Phys. Rev. A* **71** 052710
[10] Zhu C, Babb J F and Dalgarno A 2006 *Phys. Rev. A* **73** 012506
[11] Shurgalin M, Parkinson W H, Yoshino K, Schoene C and Lapatovitch W P 2000 *Meas. Sci. Technol.* **11** 730
[12] Vadla C, Beuc R, Horvatic V, Movre M, Quentmeier A and Niemax K 2006 *Eur. Phys. J. D* **37** 37
[13] Vadla C, Horvatic V and Niemax K 2006 *Appl. Phys. B* **84** 523
[14] Shindo F, Babb J F, Kirby K and Yoshino K 2007 *J. Phys. B* **40** 2841
[15] Chung H K, Kirby K and Babb J F 1999 *Phys. Rev. A* **60** 2002
[16] Chung H K, Kirby K and Babb J F 2001 *Phys. Rev. A* **63** 032516
[17] Lamoudi N, Bouledroua M, Aliou K, Allouche A R and Aubert-Frécon M 2013 *Phys. Rev. A* **87** 52713
[18] Talbi F, Bouledroua M and Aliou K 2008 *Eur. Phys. J. D* **50** 141
[19] Aubert-Frécon M *private communication*
[20] Pauly H 1979 in *Atomic–Molecule Collision Theory*, ed. Bernstein R B (New York: Plenum Press)
[21] Marinescu M and Sadeghpour R H 1999 *Phys. Rev. A* **59** 390
[22] Schmidt-Mink I, Müller W and Meyer W 1984 *Chem. Phys. Lett.* **112** 120
[23] Mabrouk N and Berriche H 2008 *J. Phys. B* **41** 155101
[24] Petsalakis I D, Tzeli D and Theodorakopoulosa G 2008 *J. Chem. Phys.* **129** 054306
[25] Kappes M M, Marti K O, Radi P, Schar M and Schumacher E 1984 *Chem. Phys. Lett.* **107** 6
[26] Engelek F, Ennen G and Meiwes K H 1982 *Chem. Phys.* **66** 391
[27] Chu X and Dalgarno A 2002 *Phys. Rev. A* **66** 024701
[28] Le Roy R J 2001 *Level v* 7.4 *Program*, *Chemical Physics Research Report*, University of Waterloo
[29] Herzberg G 1963 *Molecular Spectra and Molecular Structure Spectra of Diatomic Molecules*, Vol. I (Princeton: D. van Nostrand Co.)
[30] Landau L D and Lifshitz E M 1981 *Quantum Mechanics: Non-Relativistic Theory* (Oxford: Pergamon Press)
[31] Reho J, Higging J, Lehmann K K and Scoles G 2000 *J. Chem. Phys.* **113** 9649
[32] Carlsson J and Sturesson L 1989 *Z. Phys. D* **14** 281
[33] Voltz U and Schmoranzer H 1966 *Phys. Scr.* **T65** 48
[34] Tiemann E, Knöckel H and Richling H 1966 *Z. Phys. D* **37** 323
[35] Numerov B 1933 *Publ. Observ. Central Astrophys. Russ.* **2** 188
[36] Press W H, Flannery B P, Teukolsky S A and Vetterling W T 1987 *Numerical Recipes: The Art of Scientific Computing* (New York: Cambridge University Press)